The Sensitivity of Main-Reflector-Distortion Compensation to Deformable-Mirror Position

D. J. Hoppe[1]

The effect of deformable-mirror position on main-reflector-distortion compensation is considered through a case study. The case of a dual-shaped reflector antenna and magnifying ellipse followed by a deformable mirror and feed is considered. The effect of feed gain on the compensation is also studied. It is found that the optimum position for the deformable mirror in the beam path computed using physical optics is in excellent agreement with that predicted using simple optical models for the system and the lens law. The sensitivity of the available compensation is a function of the magnitude of the main-reflector distortion, with the location of the deformable mirror becoming more critical for larger main-reflector distortions. Increases in feed gain on the order of 3 dB from the optimum are found to have only a small impact on the effectiveness of the compensation.

I. Introduction

Gain loss due to gravity-distortion effects on a large reflector antenna can become significant for a sufficiently high operating frequency [1]. This is certainly the case for the DSN 70-meter antennas operating near 32 GHz (Ka-band). One approach for restoring the lost gain is to insert a deformable mirror in the beam path that can be distorted to counteract the main-reflector distortions and restore the lost efficiency. Recent demonstrations have indeed demonstrated gain recovery on DSS 14 using this approach [2].

There are three major factors affecting the performance of a deformable-mirror system. The first factor that will limit performance is that perfect knowledge of the true main reflector is required in order to obtain perfect compensation from the deformable mirror. Due to measurement and interpolation errors, this knowledge is never available. In general, an infinite number of actuators is required on the deformable mirror in order to obtain an arbitrary deformation. The finite number of degrees of freedom in the plate due to a finite number of actuators is the second limitation.

The third limitation, placement of the deformable mirror in the path, is the subject of this article. For a large main reflector with small distortions, the amplitude of the reflected field is essentially unaffected,

[1] Communications Ground Systems Section.

The research described in this publication was carried out by the Jet Propulsion Laboratory, California Institute of Technology, under a contract with the National Aeronautics and Space Administration.

but the phase is disturbed from the undistorted case. As the field propagates away from the main reflector, these phase distortions are partially converted into amplitude distortions through the radiation process. Therefore, at an arbitrary position in the beam path, both an amplitude and a phase correction are required. The deformable mirror can provide only a phase correction and will have limited performance at any arbitrary location due to the amplitude distortion present there.

Using simple optical models for the system and the lens law, it is possible to find the location of the image of the main reflector in the beam path. At this location, one would expect the amplitude effect to be near zero again, and this is a near-optimum location for the deformable mirror. The extent of the applicability of these simple lens models to the dual-shaped reflector system needs to be investigated. In this article, the optimum location for the mirror is found using physical optics and compared with the optical-model result. Due to constraints in the physical layout of the optical system, the optimum location may not be available. The sensitivity of this optimum location as a function of the magnitude of the main-reflector distortion is determined. Finally, the effect of feed gain on the compensation is also studied.

The results of this study will be used to determine the final location of the deformable mirror for upcoming experiments at DSS 13. In addition, the computer programs developed for the study can be used to assess the performance-versus-position characteristics of a deformable mirror on DSN 70-meter dual-shaped antennas such as DSS 14.

II. Geometry

A schematic representation of the case under consideration is shown in Fig. 1. The main-reflector and subreflector surfaces chosen are the DSS-13 shaped surfaces [3]. The main reflector has an overall diameter of 34 meters with a beam-waveguide hole in the center approximately 3 meters in diameter. The subreflector diameter is approximately 3.4 meters. The main-reflector focal length is approximately 11.8 meters, and the subreflector focal length is approximately -1.7 meters. The re-imaging ellipse has foci 7.85 and 4.2 meters from the mirror and an angle of incidence of 30 degrees. The corresponding focal length for the ellipse is 2.73 meters. The 7.85-meter focal point of the ellipse is placed on the secondary focus of the subreflector, and the phase center of the feed is placed on the 4.2-meter focal point. The deformable mirror is placed a distance "dz" in front of the feed.

Of primary interest in this article is the ability of this deformable mirror to correct for the main-reflector distortion versus its position in the beam path, dz. Using the focal lengths for the reflectors and

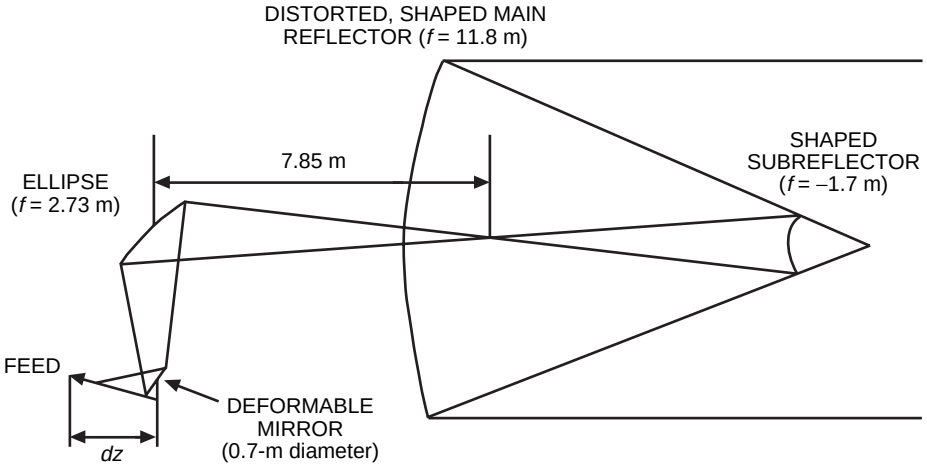

Fig. 1. Geometry for the case study.

the lens law, the final image of the main reflector is formed approximately 1 meter in front of the feed. From this simple analysis, we expect optimum performance of the deformable mirror when it is placed near this location, $dz = 1$ meter.

III. Theory

In order to evaluate the performance of the deformable mirror, an approximate analysis based on physical optics analysis is carried out. The effectiveness of the deformable mirror is determined by computing a coupling integral over the current on the mirror generated by two different excitations. The approach is similar to that described for Gaussian beams in Goldsmith [4]. The first excitation is a plane wave incident on the antenna in the boresight direction. The current induced on the distorted main reflector then reradiates to the subreflector, from there to the ellipse, and finally on to the deformable mirror, where a current, J_{pw}, results. The feed is used to provide the second excitation and resulting deformable-mirror current, J_f. If these two vector currents are complex conjugates of each other, perfect coupling occurs, and the feed will radiate with maximum efficiency in the boresight direction. Any difference in phase, amplitude, or polarization between these currents results in an efficiency loss. Definitions of the various efficiency terms and details of the efficiency calculation follow below.

The overall coupling efficiency, η_{tot}, of the incident plane wave to the feed is computed on the surface of the deformable mirror using the following formula:

$$\eta_{tot} = \frac{|C_{FPW}|}{\sqrt{P_F^{tot}}\sqrt{P_{PW}^{tot}}}$$

The complex coupling integral in the numerator of this expression is given by

$$C_{FPW} = \iint\limits_{\text{mirror}} \bar{J}_{PW} \bullet \bar{J}_F ds$$

and the normalization integrals in the denominator are

$$P_F^{tot} = \iint\limits_{\infty} \bar{J}_F^* \bullet \bar{J}_F ds$$

and

$$P_{PW}^{tot} = \iint\limits_{\infty} \bar{J}_{PW}^* \bullet \bar{J}_{PW} ds$$

The normalization integrals are carried out over a fictional surface large enough to capture all the significant energy in the plane wave and feed fields.

The first factor that limits the efficiency of the deformable mirror is its finite extent. To isolate this effect, the total efficiency is broken into a coupling efficiency based upon use of only the plate currents and a spillover efficiency defined by the following equations:

$$\eta_{tot} = \eta_C \eta_{\text{spill}}$$

$$\eta_{\text{spill}} = \frac{\sqrt{P_F}\sqrt{P_{PW}}}{\sqrt{P_F^{tot}}\sqrt{P_{PW}^{tot}}}$$

$$P_F = \iint\limits_{\text{mirror}} \bar{J}_F^* \bullet \bar{J}_F ds$$

and

$$P_{PW} = \iint\limits_{\text{mirror}} \bar{J}_{PW}^* \bullet \bar{J}_{PW} ds$$

The term η_c has the same form as η_{tot} but with the normalization carried out over the mirror only.

The available coupling efficiency from an idealized deformable mirror, η_{avail}, can be computed using

$$\eta_{\text{avail}} = \eta_A \eta_{\text{spill}}$$

where the amplitude efficiency, η_A, is given by

$$\eta_A = \frac{\left|C_{FPW}^A\right|}{\sqrt{P_F}\sqrt{P_{PW}}}$$

and

$$C_{FPW}^A = \iint\limits_{\text{mirror}} \bar{J}_{PW} \bullet \bar{J}_F e^{j\phi(s)} ds$$

In the last equation, $\phi(s)$ is the adjustable phase imparted to the coupling process through deforming an idealized deformable mirror. The computer model of the deformable mirror is made up of a finite number of triangular facets. The adjustable phase is chosen on a triangle-by-triangle basis in order to maximize the above integral. The mirror is idealized in the sense that no consideration is given to the physical realization of this phase adjustment, the smoothness of the surface, the number of actuators required, etc.

If the ratio of the uncorrected coupling efficiency to this ideal phase-corrected efficiency is defined as the phase efficiency, η_ϕ, then the overall coupling efficiency may be factored as

$$\eta_{tot} = \eta_A \eta_\phi \eta_{\text{spill}}$$

The spillover efficiency can approach unity for a large enough deformable mirror placed anywhere in the beam path. It will be seen in the following section that the product of phase efficiency, η_ϕ, and amplitude efficiency, η_A, is roughly independent of the position of the deformable mirror. The distribution between phase and amplitude efficiency does depend on the position of the mirror. Investigation of this dependence is the subject of the next section. In order to compute the available efficiency from an idealized deformable mirror, the phase efficiency term above is simply replaced by unity. It will be shown that it is possible to find a mirror position where nearly all of the inefficiency is concentrated in the phase term and therefore can be recovered completely by an idealized deformable mirror.

IV. Results

For this case study, a smoothed version of the distortion obtained using holography at DSS 13 for an elevation angle of 12.7 degrees was used. The surface height distortion is plotted in Fig. 2. Although the scale of the plot covers ±3 mm, all of the extreme excursions are located on the rim of the reflector. The rms path-length error represented on the surface is much smaller, approximately 0.4 mm. This distortion was then amplified by factors of two and three in order to evaluate the performance characteristics of the deformable-mirror system for main-reflector distortions resulting in more significant gain loss. All of the physical optics calculations were carried out at 32 GHz.

Figure 3 shows the various efficiency factors for an undistorted main-reflector-versus-deformable-mirror position and a feed gain of 22.37 dBi. Figure 4 repeats these calculations for a feed gain of 26.0 dB. For positions near the feed, the overall efficiency is dominated by how well feed current matches the plane-wave current. The overall efficiency approaches 97 percent for the 22-dBi feed and 95 percent for the 26-dBi feed. These high values are expected since the antenna surfaces have been shaped to maximally couple a 22.37-dBi feed to the plane wave. The slight drop in efficiency from the use of a 26-dB feed is also in agreement with expectations. For large feed-to-deformable-mirror distances, the loss is dominated by spillover, and the 26-dB feed gives the best performance despite its imperfect match to the plane-wave currents.

Figure 5 shows the efficiencies computed using a 22.37-dBi feed and the 12.7-degree elevation distortion. The overall efficiency is the efficiency computed assuming no phase compensation whatsoever. The available efficiency is that available using a perfect phase-compensating deformable mirror. Amplitude, phase, and spillover efficiencies are also indicated on the figure. The product of the amplitude and phase efficiency in this case is approximately 77 percent. The amplitude efficiency peaks near a deformable-mirror position of 1 meter at a value of 98 percent. At this position, an overall efficiency of 94 percent can be reached using an ideal deformable mirror. Due to spillover effects, the highest absolute efficiency available from the mirror is 95.5 percent, reached at 76 cm. For mirrors placed closer to the feed than 76 cm, amplitude error dominates the performance, and, for values greater than 1 m, spillover dominates.

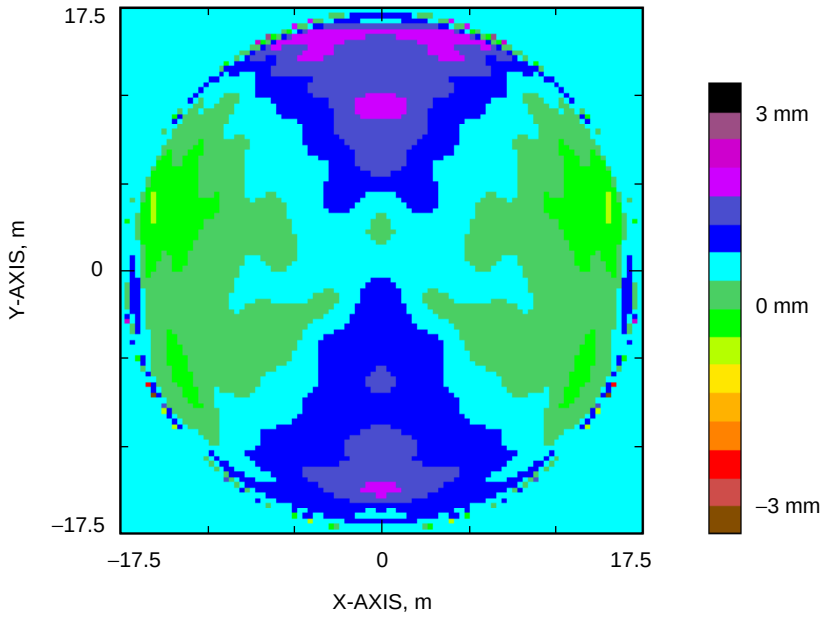

Fig. 2. The main-reflector distortion used in the case study.

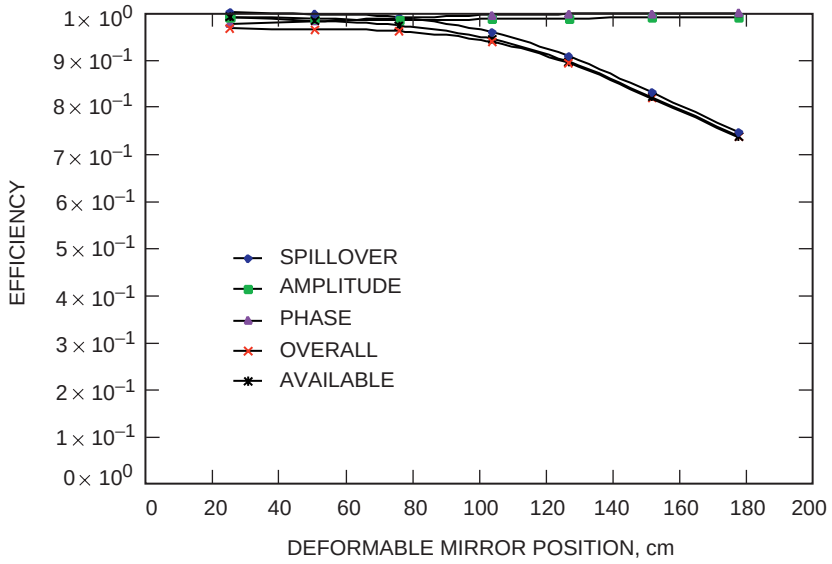

Fig. 3. Efficiency: undistorted main reflector, 22.37-dBi feed.

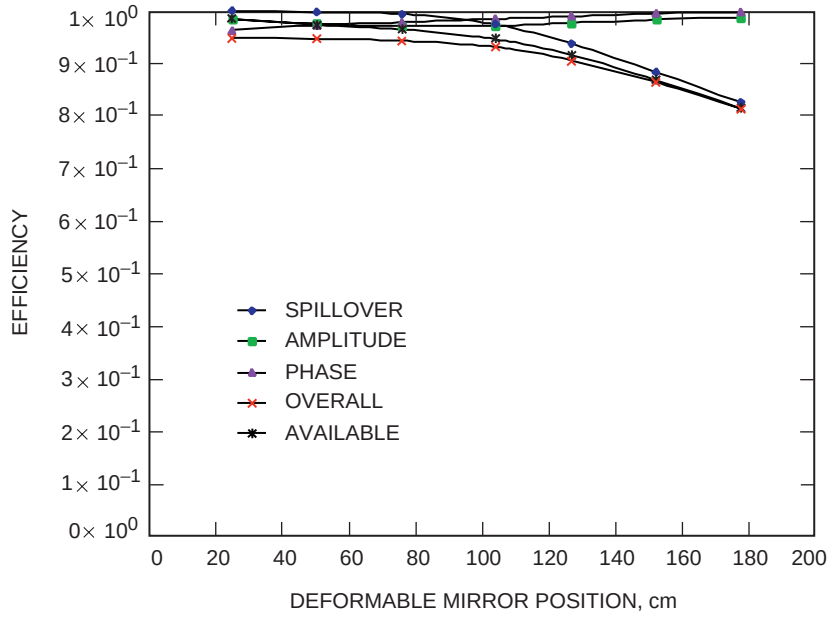

Fig. 4. Efficiency: undistorted main reflector, 26.0-dBi feed.

Figures 6 through 12 present the computed currents on the deformable mirror for the various mirror positions used to create Fig. 5. In each case, the magnitude of the current is normalized to its peak, and a 26-dB range is plotted. As the distance from the feed to the deformable mirror increases, the increased spillover is evident. It is also obvious that the best amplitude match between the plane wave and feed currents is at $dz = 104$ cm. The amplitude match is better for larger values of dz than for smaller values. For large dz, both the feed and plane-wave currents become more uniform at the expense of spillover. These characteristics are represented in the efficiency values presented in Fig. 5.

Figure 13 shows the efficiencies computed using a 22.37-dBi feed and the 12.7-degree elevation distortion scaled by a factor of two. The product of the amplitude and phase efficiency in this case is

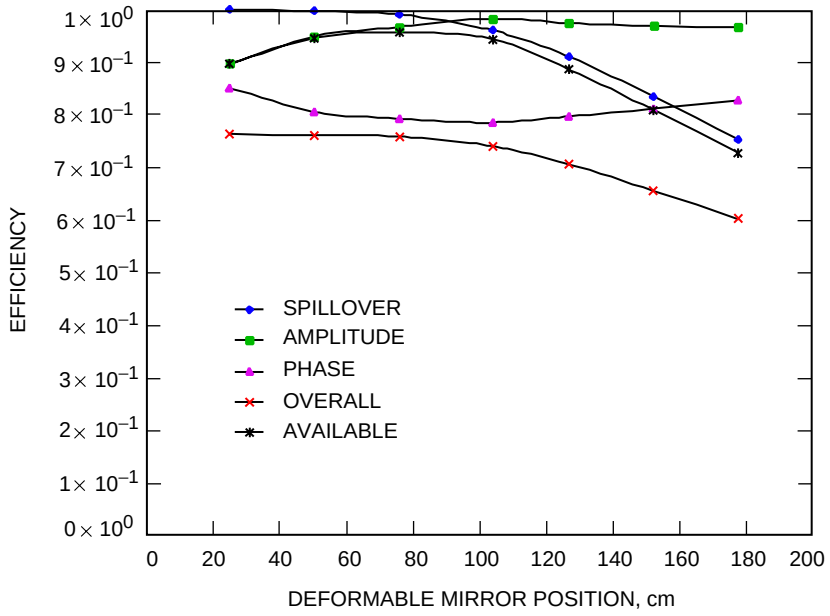

Fig. 5. Efficiency: 12.7-deg distortion, 22.37-dBi feed.

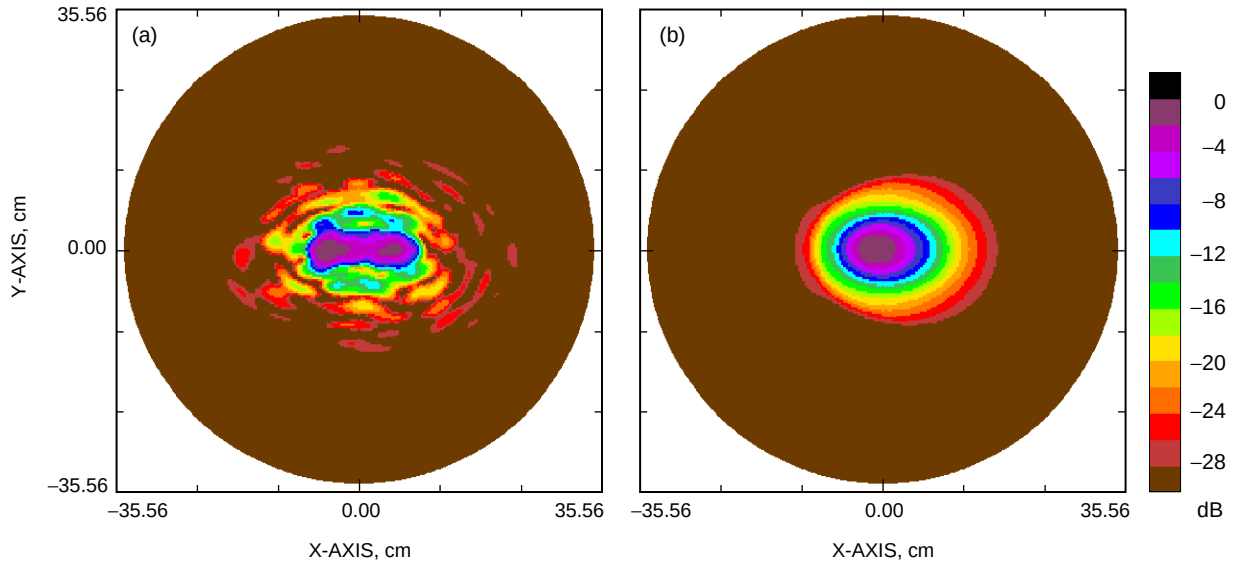

Fig. 6. Deformable mirror currents *dz* = 25.4 cm: (a) plane wave and (b) 22.37-dBi feed.

approximately 34 percent. In this case, the amplitude efficiency peaks near a deformable-mirror position of 1 meter at a value of 97 percent, slightly lower than the 98 percent value for the smaller-distortion case. At this position, an overall efficiency of 93.5 percent can be reached using an ideal deformable mirror. In this case, the performance of the deformable mirror versus position has a more rapid roll-off than the lower distortion case of Fig. 5, a trend that will continue for larger distortions.

Figure 14 shows the efficiencies computed using a 22.37-dBi feed and the 12.7-degree elevation distortion scaled by a factor of three. The product of the amplitude and phase efficiency in this case is approximately 14 percent. Once again the amplitude efficiency peaks near a deformable-mirror position of 1 meter at a value of 95.5 percent, slightly lower than previous cases. At this position, an overall efficiency of 92 percent can be reached using an ideal deformable mirror.

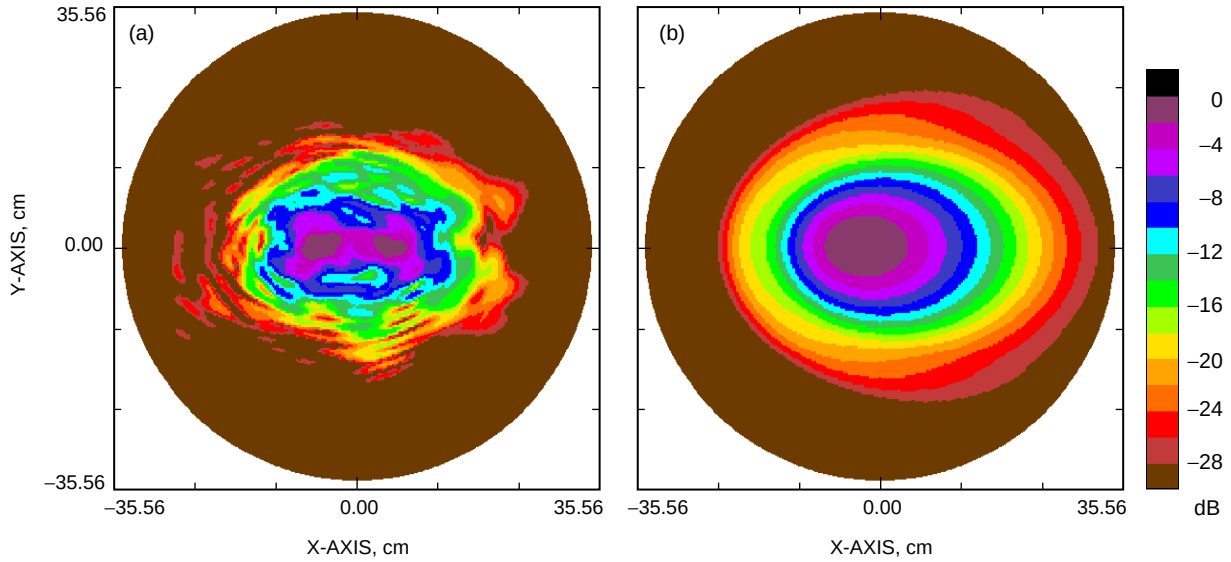

Fig. 7. Deformable mirror currents *dz* = 50.8 cm: (a) plane wave and (b) 22.37-dBi feed.

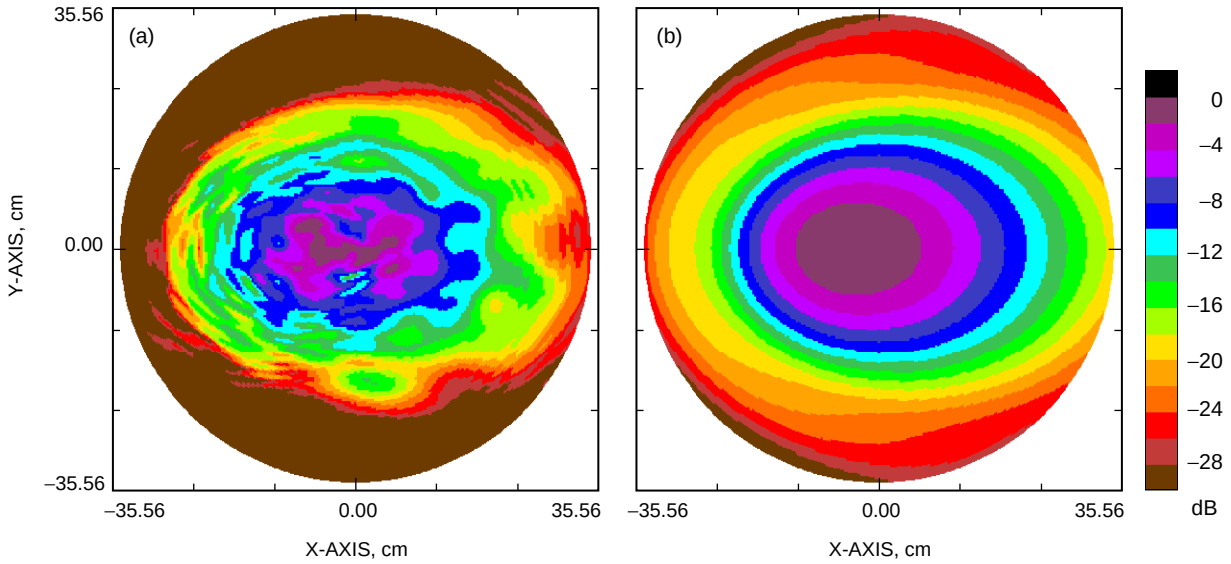

Fig. 8. Deformable mirror currents *dz* = 76.2 cm: (a) plane wave and (b) 22.37-dBi feed.

Figure 15 repeats the above case using a 26-dBi feed instead of the 22.37-dBi feed. The results are quite similar, with only minor differences for large and small mirror distances. These results indicate that the deformable-mirror performance is quite insensitive to the gain of the feed.

Figures 16 and 17 summarize the amplitude efficiency and available efficiency, the product of amplitude efficiency and spillover efficiency, for the various distortions studied and a 22.37-dBi feed. Both efficiencies peak near a mirror position of 1 meter, as expected from the simple optical analysis. The efficiency peak as well as the width of the curves is reduced as the distortion increases.

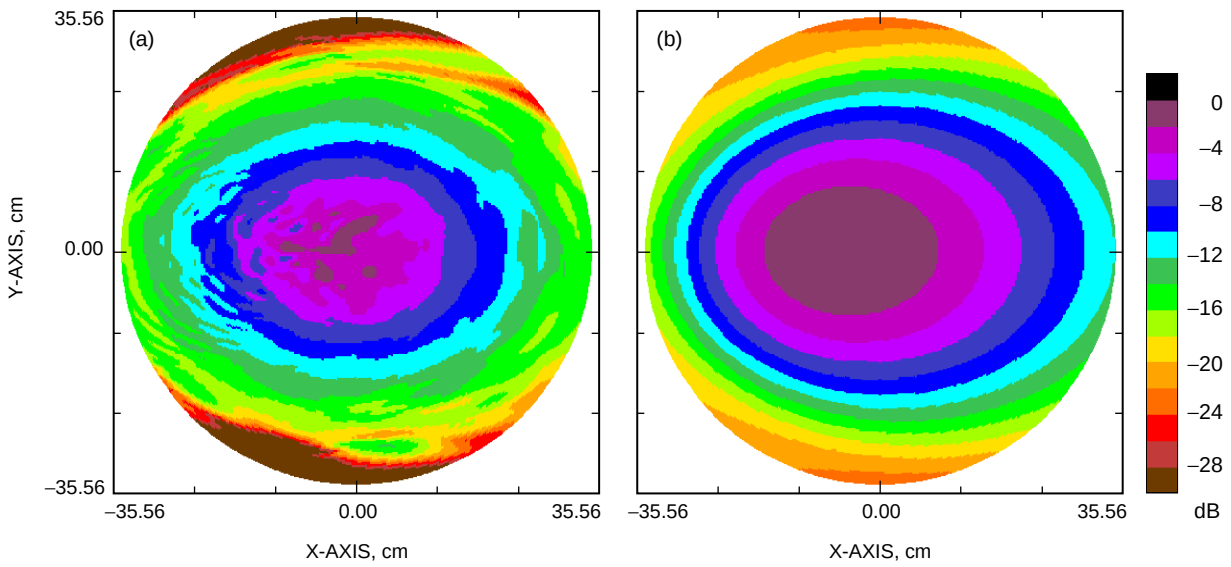

Fig. 9. Deformable mirror currents *dz* = 104 cm: (a) plane wave and (b) 22.37-dBi feed.

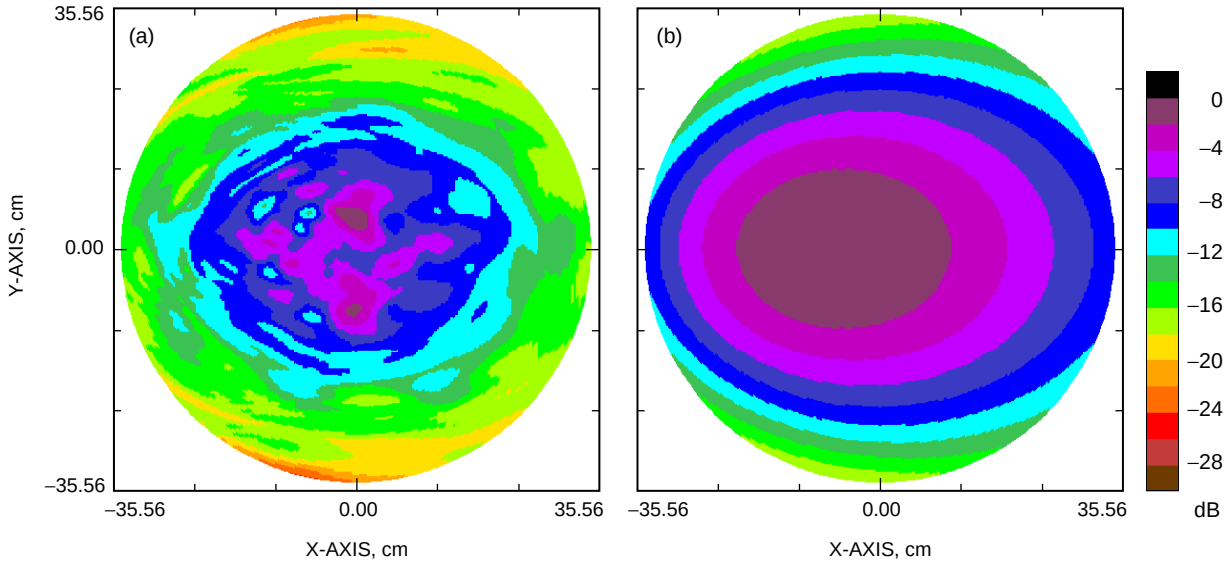

Fig. 10. Deformable mirror currents *dz* = 127 cm: (a) plane wave and (b) 22.37-dBi feed.

V. Conclusions

The case study has shown that the optimum position for the deformable mirror in the beam path is in excellent agreement with that predicted by a simple optical analysis using ideal lens models for the system. Various efficiency factors have been defined and computed for several levels of main-reflector distortion-versus-deformable-mirror location. The overall level of compensation available from the deformable mirror is slightly reduced as the main-reflector distortion increases. The sensitivity of the performance of the mirror to its position in the beam path also increases as the main-reflector distortion increases.

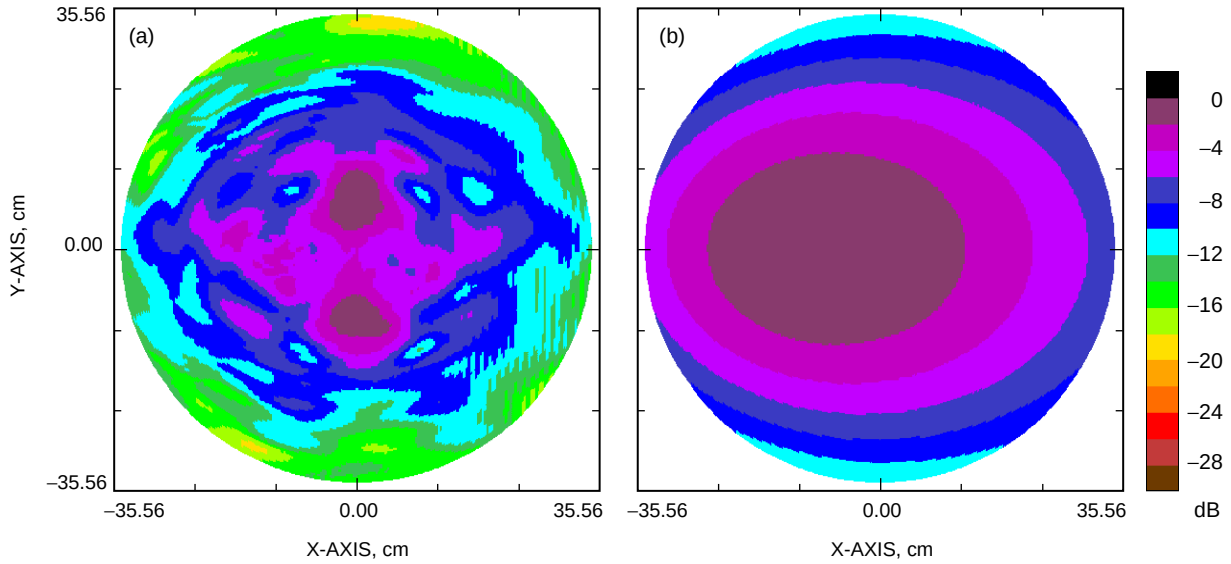

Fig. 11. Deformable mirror currents *dz* = 154 cm: (a) plane wave and (b) 22.37-dBi feed.

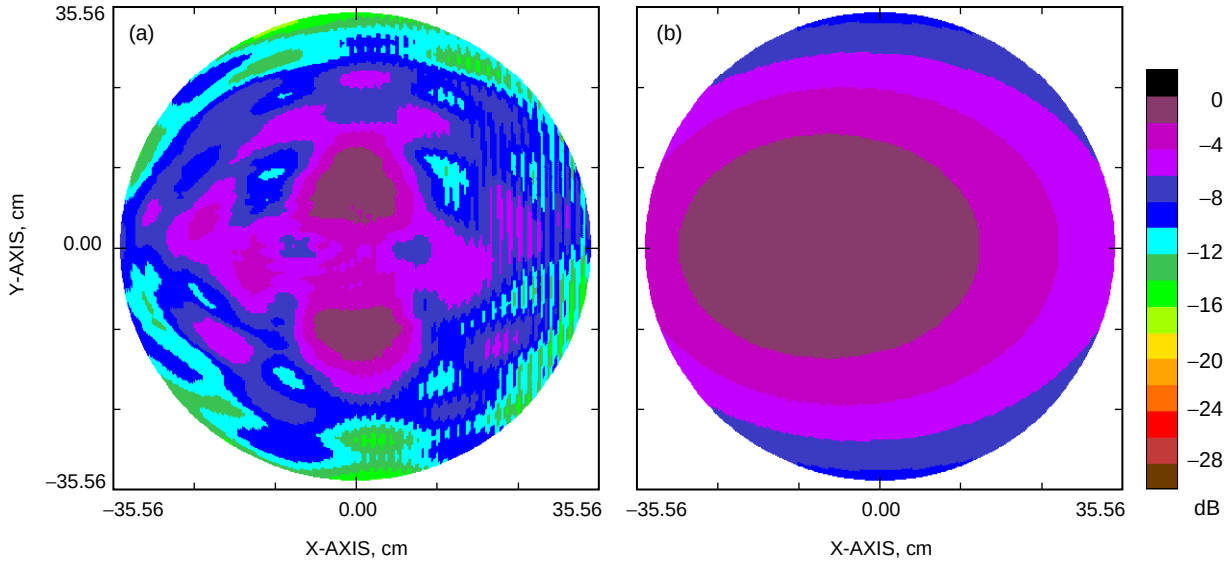

Fig. 12. Deformable mirror currents *dz* = 178 cm: (a) plane wave and (b) 22.37-dBi feed.

When implementing a deformable-mirror system, an effort should be made to place the mirror in the optimum position in the beam path. In this position, the efficiency is optimum and the required mirror deformation closely resembles the main-reflector distortion. Any physical realization of the deformable mirror will be unable to achieve the performance of the idealized mirror used to generate the results in this article. Even at the optimum position, a deformable mirror with a finite number of actuators will fall short of the optimum performance. In addition, the sensitivity of its performance to position in the beam path may differ from the results presented here for an idealized deformable mirror.

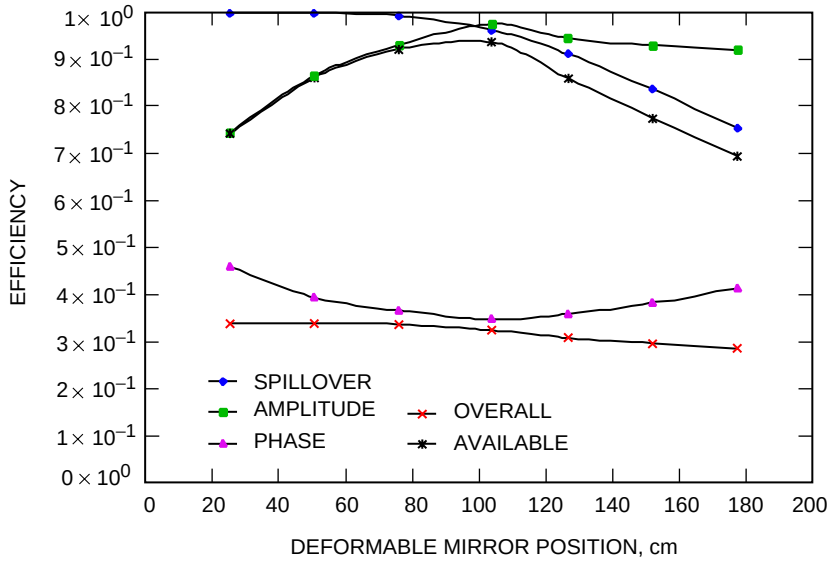

Fig. 13. Efficiency: 12.7-deg distortion, amplitude doubled, 22.37-dBi feed.

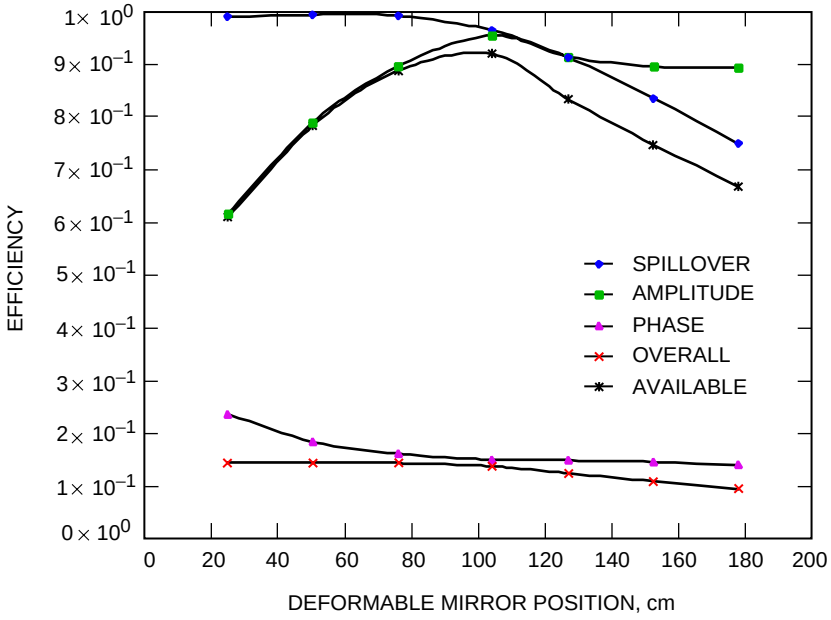

Fig. 14. Efficiency: 12.7-deg distortion, amplitude tripled, 22.37-dBi feed.

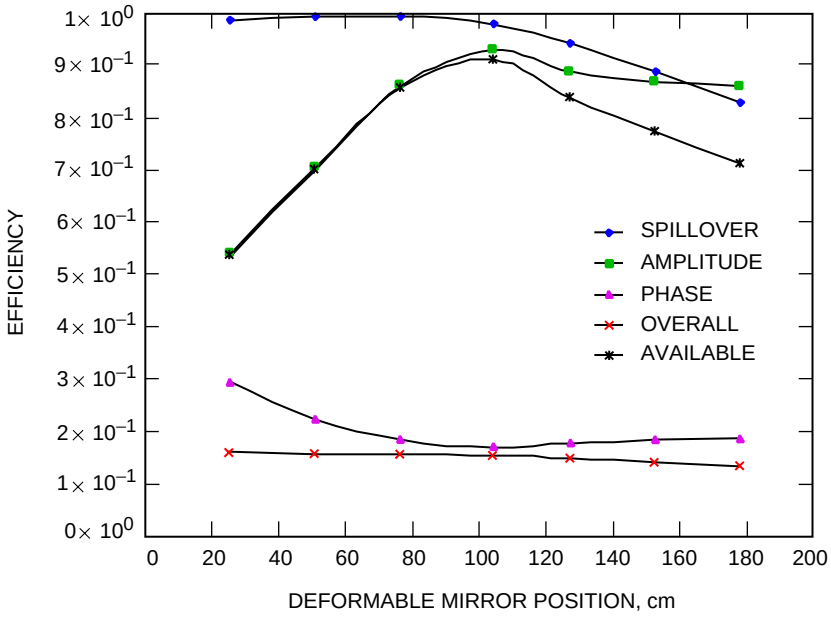

Fig. 15. Efficiency: 12.7-deg distortion, amplitude tripled, 26.0-dBi feed.

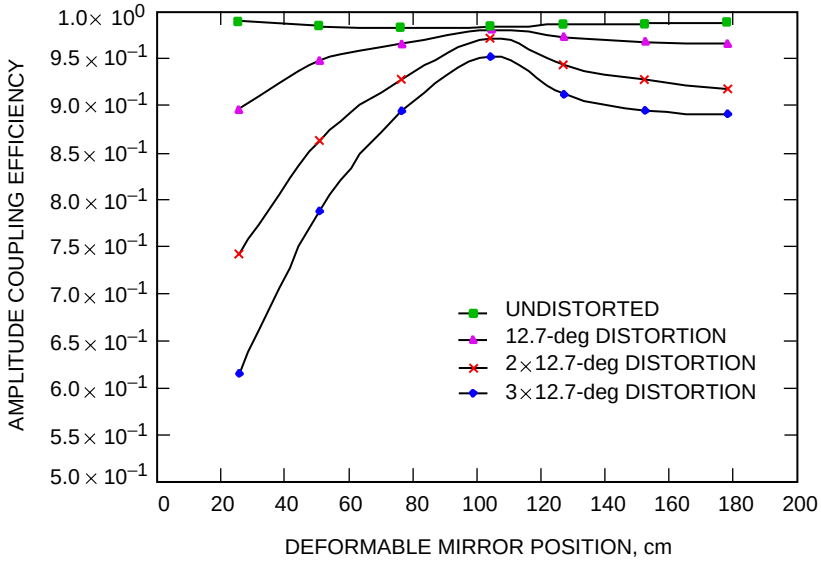

Fig. 16. Amplitude efficiency versus deformable-mirror position.

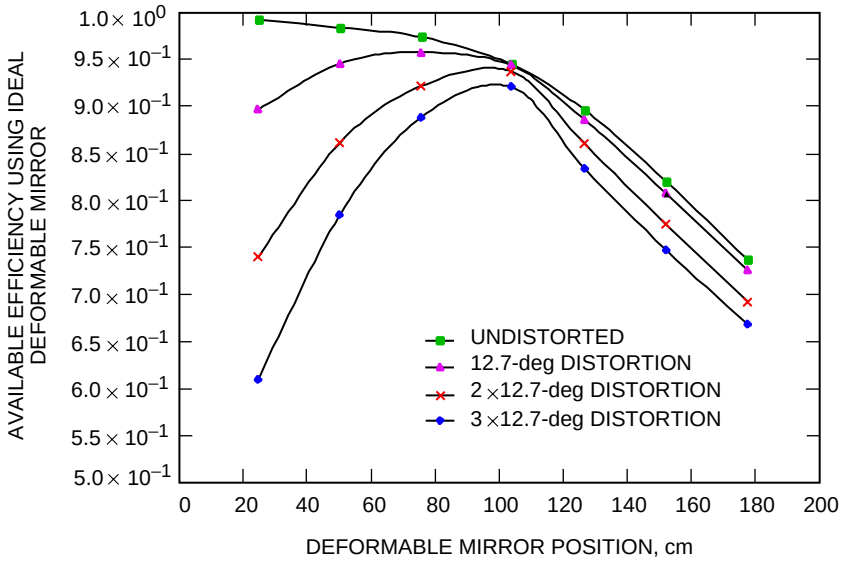

Fig. 17. Available efficiency versus deformable-mirror position.

References

[1] S. D. Slobin, *DSN/Flight Project Interface Design Handbook*, JPL 810-5, Rev. D, vol. I, "DSN Telecommunications Interfaces 70 Meter Antenna Subnet," TCI-10, Rev. G, Jet Propulsion Laboratory, Pasadena, California, January 15, 1997.

[2] P. Richter, M. Franco, and D. Rochblatt, "Data Analysis and Results of the Ka-Band Array Feed Compensation System–Deformable Flat Plate Experiment at DSS 14," *The Telecommunications and Mission Operations Progress Report 42-139, July–September 1999*, Jet Propulsion Laboratory, Pasadena, California, pp. 1–29, November 15, 1999.
http://tmo.jpl.nasa.gov/tmo/progress_report/42-139/139H.pdf

[3] W. Veruttipong, W. Imbriale, and D. Bathker, "Design and Performance Analysis of the DSS-13 Beam Waveguide Antenna," *The Telecommunications and Data Acquisition Progress Report 42-101, January–March 1990*, Jet Propulsion Laboratory, Pasadena, California, pp. 99–113, May 15, 1990.
http://tmo.jpl.nasa.gov/tmo/progress_report/42-101/101H.PDF

[4] P. F. Goldsmith, *Quasioptical Systems*, New York: IEEE Press, 1998.